RSC Advances

PAPER

View Article Online
View Journal | View Issue

Open Access Article. Published on 17 March 2017. Downloaded on 10/17/2025 1:37:14 AM.
This article is licensed under a Creative Commons Attribution 3.0 Unported Licence.

Cite this: *RSC Adv.*, 2017, 7, 17095

# Investigations on the mechanism, kinetics and isotherms of ammonium and humic acid co-adsorption at low temperature by 4A-molecular sieves modified from attapulgite†

Nan Sun,*[a] Wenxin Shi,[b] Lixin Ma[c] and Shuili Yu*[bd]

Attapulgite (ATP) is a type of natural magnesium aluminum silicate mineral and has been applied as an adsorbent to remove organic pollutants and heavy metals in aqueous solution. This study investigated the 4A-molecular sieve modified from ATP on simultaneous adsorption of ammonium and humic acid (HA). The properties of raw and alkali treated ATP were compared such as surface morphologies, crystallinity phase and removal efficiency. The influences of 4A-molecular sieve dosage, pH values, mixing speed, initial contaminants' concentration, solution temperature and adsorption time on removal of ammonium and HA were thoroughly evaluated. The results indicated that the removal efficiency of ammonium at the low temperature of 5 °C increased dramatically using alkali modified ATP comparing with that using the raw ATP. The optimum 4A-molecular sieve dose was 1 g $L^{-1}$ and the maximum adsorption of ammonium was obtained at natural water's pH, while the maximum HA adsorption was obtained at around pH 4. The adsorption isotherms and kinetics for adsorption of ammonium and HA were also studied to obtain the adsorption mechanisms. It was found that the temperature did not have a significant influence on the removal of ammonium and HA. The ammonia has likely been removed from water through electrostatic adsorption and ion-exchange whereas the humic acid might be eliminated *via* a mechanism of electrostatic adsorption and cation-bridge effect. These results revealed that 4A-molecular sieves modified from ATP have a significant potential for applications of ammonium removal at low temperature.

Received 7th January 2017
Accepted 13th March 2017

DOI: 10.1039/c7ra00268h

rsc.li/rsc-advances

## 1. Introduction

In the northeast of China, surface water with low temperatures (below 10 °C in winter) is one of the main drinking water sources, however, the presence of ammonium and natural organic matters (NOM) in the surface water bodies could cause taste, odor and color problems.[1,2] The high concentration of ammonium in water could lead to eutrophication and formation of nitrite in the distribution systems.[3] The ammonia in water sources can also interfere with the chlorination processes and decrease the disinfection efficiency.[4] Humic acids (HA) which are assemblages of high molecular weight natural polymers constitute the NOM.[5] Their surface functional groups like carboxyl (–COOH) and phenolic hydroxyl (–OH) groups are attached to aromatic rings, thus they are anionically hydrophobic in water sources.[6,7] During the disinfection and chlorination of drinking water, HA could form strong toxic disinfection byproducts (DBPs) such as trihalomethanes (THMs) which is also carcinogenic.[8] It is therefore essential to eliminate ammonium and HA from water before supplying it for drinking to maintain human health.

Many drinking water treatment approaches such as coagulation/flocculation, sedimentation, ion exchange, biodegradation, filtration and so on have been applied to remove ammonium and HA from water, however their efficiency is not high especially at low temperature. Adsorption has the advantages of simplicity and high efficiency for elimination of ammonium and HA, so more and more attentions have been paid for its investigation. Zeolite,[1,3,9–13] clay minerals,[14–17] fly ash,[18,19] activated carbons,[20] and chitosan[21] have been investigated as adsorbents, of which clays are more attractive because of their high mechanical and chemical stability as well as low cost.

[a]School of Water Conservancy and Civil Engineering, Northeast Agricultural University, Harbin 150030, China. E-mail: nan662001@163.com; Fax: +86 21 65982708; Tel: +86 21 65982708

[b]State Key Laboratory of Urban Water Resource and Environment, Harbin Institute of Technology, Harbin 150090, China. E-mail: yu_shuili@163.com

[c]Department of Environmental Protection of Heilongjiang Province, Harbin 150090, China

[d]State Key Laboratory of Pollution Control and Resources Reuse, Tongji University, Shanghai 200092, China

† Electronic supplementary information (ESI) available. See DOI: 10.1039/c7ra00268h

Open Access Article. Published on 17 March 2017. Downloaded on 10/17/2025 1:37:14 AM.
This article is licensed under a Creative Commons Attribution 3.0 Unported Licence.

Attapulgite (ATP), which is a type of natural magnesium aluminum silicate mineral, has a porous structure, large specific surface area and moderate cation exchange capacity.[22] It has been applied as adsorbents to remove organic pollutants and heavy metal in aqueous solution.[23] However, the adsorption efficiency and capacity of ATP are not high enough to meet the demand in practice, so modifications of ATP need to be investigated to remove organic contaminants, ammonium and heavy metal efficiently. It has been reported that organic modified ATP with polymers or small molecules have been explored to improve the characterizations and properties of ATP.[23,24] However, other modification methods like alkali treatment for ATP have been rarely conducted and reported. In this study, ATP was modified by alkali treatment to 4A-molecular sieve as adsorbents to remove ammonium and HA simultaneously. And the effects of molecular sieve concentration, solution pH, temperature and mixing speed on removal of ammonium and HA were investigated as single and binary component.

## 2. Materials and methods

### 2.1 Materials

In the experiments, the ATP with an average particle size of 200-mesh screen was obtained from Xu Yi in Jiang Su province, China and the main components of ATP were shown in Table 1. The compaction density of ATP is 0.8–0.9 g $mL^{-1}$, and the pH is around 6.5–8.0. Before experiments, the raw ATP was washed with distilled water and then dried at 105 °C. The $NH_4Cl$ and HA were dissolved into distilled water to prepare the solutions for adsorption, and all of the chemicals used in the experiments were analytical grade.

### 2.2 Alkali treatment

The clean and dry ATP was put into NaOH solution with a concentration of 0.5 mol $L^{-1}$, and then mixed with a rotation speed of 200 rpm, 100 °C. After filtration, the alkali solution containing $Na_2SiO_3$ was obtained. Given percentages of $NaAlO_2$, NaOH and $H_2O$ ($n(Na_2O)/n(SiO_2) = 2.1$, $n(H_2O)/n(Na_2O) = 60$, $n(SiO_2)/n(Al_2O_3) = 1.5$) were added into the alkali solution, and the solution was mixed at 25 ± 5 °C for 1 h to form the silicon aluminate gel which crystallized at 90 °C for 12 h in reaction kettle. The crystal was washed with distilled water and then dried to obtain the 4A-molecular sieve.

### 2.3 Adsorption experiments

The adsorption properties of raw and modified ATP were characterized by batch experiments. In each experiment, 100 mL of solution with different concentrations of HA (and/or $NH_4Cl$) were adjusted to the desired value of pH with 0.1 mol $L^{-1}$ NaOH or HCl and transferred into the conical flask with a volume of 250 mL. Then a certain amount of raw or modified ATP was added into the conical flask. The mixture was stirred at 200 rpm for a given time and was centrifuged at 4000 rpm for 10 min. The supernatant then passed through the 0.45 μm microfiltration membrane and the concentration of HA (and/or $NH_4Cl$) was analyzed from the filtrate. The adsorption capacity $q_e$ (mg $g^{-1}$) can be calculated *via* the following equation:

$$q_e = \frac{(C_0 - C_e)V}{M} \quad (1)$$

where $V$ (L) was the volume of HA (and/or $NH_4Cl$) solution, $C_0$ and $C_e$ (mg $L^{-1}$) were the concentration of HA (and/or $NH_4Cl$) solution before and after adsorption, respectively, and $M$ (g) was the adsorbent weight.

The percentage removal $R$ (%) of HA (and/or $NH_4Cl$) was calculated by the following equation:

$$R = \frac{(C_0 - C_e)}{C_e} \times 100\% \quad (2)$$

The 4A-molecular sieve dosage, pH value of solution, initial concentration of contaminant(s), mixing speed and temperature were selected as variables in this study.

In the experiments for the effects of initial contaminants' concentration on adsorption, the initial concentrations of $NH_4Cl$ as single contaminant were: 1, 3, 5, 8, 10, 20, 40, 60, 80 and 100 mg $L^{-1}$, the initial concentrations of HA as single contaminant were: 1, 2, 3, 5, 6, 8, 10, 15 and 20 mg $L^{-1}$, and the initial concentrations of binary contaminants were 3 : 1, 5 : 2, 8 : 3, 10 : 5, 20 : 6, 40 : 8, 60 : 10, 80 : 15 and 100 : 20 ($C_{NH_4Cl}$ : $C_{HA}$, mg $L^{-1}$ : mg $L^{-1}$).

### 2.4 Characterization

The raw and modified ATP were characterized by scanning electron microscope (SEM, Quanta FEG200), X-ray diffraction (XRD, D/max-rB 12 KW) and X-Ray Spectrometer (XRF, AXIOS-PW4400) for analyzing the surface morphology, the crystallinity phase and the chemical composition, respectively. The pH drift procedure was applied to determine the pH of zero charge point ($pH_{zpc}$).[1]

The concentration of HA was determined by a UV-vis spectrometer (T6 New century) with detecting wavelength at 254 nm. The Nessler's reagent colorimetric method was used to measure the concentration of ammonia in solution including ionized ($NH_4^+$) and non-ionized ($NH_3$) species. The equivalent concentrations of cations in the solution before and after reaction in the molecular sieve-solution system were measured by Inductively Coupled Plasma-Atomic Emission Spectrometry(ICP-AES-5300DV, PE, USA) to investigate the ion exchange degree. The

Table 1 Main components and content of the oxides for original attapulgite from Xu Yi

| Component | $SiO_2$ | $Al_2O_3$ | $Fe_2O_3$ | MgO | $K_2O$ | $TiO_2$ | CaO | $SO_3$ | $Na_2O$ |
|---|---|---|---|---|---|---|---|---|---|
| Content (%) | 69.171 | 10.552 | 5.507 | 12.869 | 1.451 | 0.695 | 1.398 | 0.644 | 0.113 |

Open Access Article. Published on 17 March 2017. Downloaded on 10/17/2025 1:37:14 AM.
This article is licensed under a Creative Commons Attribution 3.0 Unported Licence.

solution after reaction was treated by suction filtration, and the filtrate was diluted and tested by ICP-AES.

# 3. Results and discussion

## 3.1 Characterization of samples

A complete characterization of raw and alkali treated ATP was carried out and the results are shown below.

**3.1.1 Surface morphology obtained by SEM scans.** The surface morphologies of original and alkali treated ATP were shown in Fig. 1. It can be seen from Fig. 1a that the original ATP had a compact structure, a small amount of space, and crystals in rod shape with a diameter ranging from 20 to 70 nm. The alkali treated ATP (Fig. 1b) had cubic and octahedral particles, and the particle diameter was around 1.75–2.5 μm, which indicated that the structure became loose and the effective specific surface area increased after the alkali treatment.

**3.1.2 Crystallinity phase obtained by XRD.** The XRD patterns of original and alkali treated ATP were shown in Fig. 2. The characteristic XRD peak of ATP was at $2\theta = 8.46°$ in Fig. 2(a).[25] After alkali treatment, the intensity of that peak became weak, and the characteristic XRD peaks of 4A-molecular sieve (at $2\theta = 7.1°$, 10.4°, 12.4° and 16.2°) were observed obviously in Fig. 2b, which indicated that the particles formed after alkali treatment of ATP were 4A-molecular sieve.

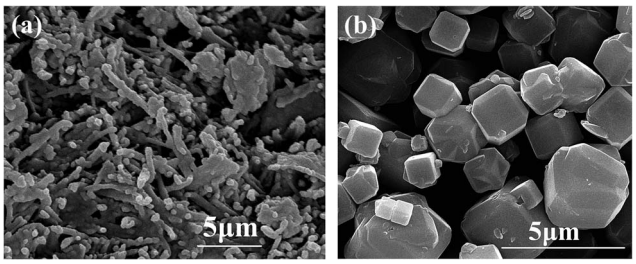


Fig. 1 SEM surface micrographs of (a) original and (b) alkali treated ATP.

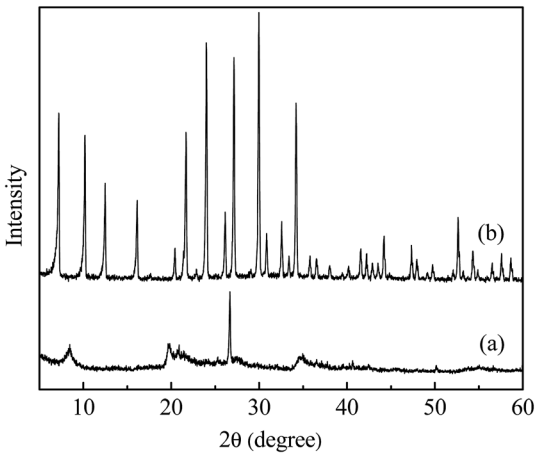


Fig. 2 XRD patterns of (a) original ATP and (b) alkali treated ATP.

**3.1.3 Chemical compositions obtained by XRF.** The chemical compositions of 4A-molecular sieve obtained by XRF were shown in Table 2. It was shown that the 4A-molecular sieve contained various cations including $Na^+$, $K^+$, $Fe^{3+}$ and $Ca^{2+}$, in which the content of $K^+$, $Fe^{3+}$ and $Ca^{2+}$ was lower than that of $Na^+$ (49.16%), therefore $Na^+$ was the most active cation involved in the ion exchange process.

## 3.2 Comparisons of removal efficiency between original and alkali modified ATP

The removal efficiency of ammonium and HA by original and alkali modified (4A-molecular sieve) ATP at low temperature was compared and the results were listed in Table 3. As seen in this table, the removal efficiency of ammonium increased dramatically (from 8.33% to 100%) after alkali modification of ATP which was attributed to the high capability of cation exchange, molecular sieving and adsorption of 4A-molecular sieve.[1] However, the removal efficiency of HA decreased (from 19.57% to 8.20%) after alkali treatment of ATP, which may be caused by the changes of $pH_{zpc}$. The $pH_{zpc}$ of ATP was 5.21, while the $pH_{zpc}$ of 4A-molecular sieve was 4.11 (displayed in Fig. S1 of ESI†). In the experimental conditions (pH = 7), the 4A-molecular sieve was negatively charged which was only attractive and exchangeable to cations.

## 3.3 The effects of 4A-molecular sieve dose on adsorption

The effects of 4A-molecular sieve dose on adsorption capacity and removal efficiency of ammonia were investigated in this study, and the contaminants were single ammonium (5 mg $L^{-1}$) and ammonium (5 mg $L^{-1}$) in the presence of HA (2 mg $L^{-1}$). The data were depicted in Fig. 3. The removal efficiency of

Table 3 Removal efficiency of ammonium and HA by ATP and 4A-molecular sieve[a]

| Adsorbent | Removal efficiency (%) | |
|---|---|---|
| | Ammonium | HA |
| ATP | 8.33 ± 0.12 | 19.57 ± 0.20 |
| 4A-molecular sieve | 99.00 ± 0.10 | 8.20 ± 0.11 |

[a] Conditions: temperature, 5 °C; pH 7; adsorbent concentration, 1 g $L^{-1}$; $NH_4Cl$, 5 mg $L^{-1}$; HA, 5 mg $L^{-1}$; contact time, 180 min; mixing speed, 200 rpm.

Table 2 Chemical compositions of the 4A-molecular sieve

| Compound (%) | $Na_2O$ | $Al_2O_3$ | $SiO_2$ | $SO_3$ | $P_2O_5$ | $K_2O$ | $Fe_2O_3$ | CaO | LOI |
|---|---|---|---|---|---|---|---|---|---|
| 4A-molecular sieve | 49.16 | 26.55 | 23.34 | 0.14 | 0.12 | 0.03 | 0.03 | 0.01 | 0.64 |

Open Access Article. Published on 17 March 2017. Downloaded on 10/17/2025 1:37:14 AM.
This article is licensed under a Creative Commons Attribution 3.0 Unported Licence.

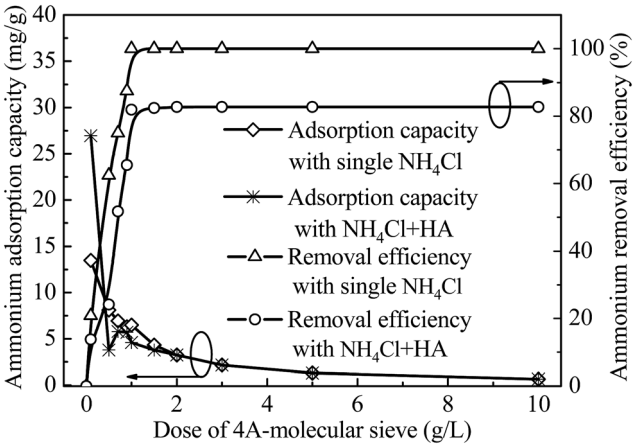


Fig. 3 The effects of 4A-molecular sieve dose on adsorption capacity and removal efficiency of ammonium with single ammonium and ammonium in the presence of HA. (Conditions: temperature, 5 °C; pH 7; contact time, 180 min; mixing speed, 200 rpm).

ammonium increased with the addition of 4A-molecular sieve doses and then reached to an equilibrium value when the dose was higher than 1 g $L^{-1}$, which indicated that the dose of 1 g $L^{-1}$ was the optimum 4A-molecular sieve dose both for single ammonia and ammonia in the presence of HA. The removal efficiency of ammonium was influenced by the presence of HA that the removal efficiency of ammonium decreased around 15% and the adsorption capacity decreased slightly. It may be caused by two reasons: (1) the negatively charged HA adsorbed the $NH_4^+$ ions by electrostatic attraction and (2) HA was adsorbed on the surface of 4A-molecular sieve which blocked the adsorption sites for ammonium.

### 3.4 The effects of pH on adsorption and the adsorption mechanism

The effects of solution pH (ranging from 2 to 12) on removal efficiency of ammonium (Fig. 4a) and HA (Fig. 4b) by 4A-molecular sieve were evaluated as both single and binary contaminants. Fig. 4a showed that in the single ammonia solution when pH increased from 2 to 7, the ammonium removal efficiency increased from 71% to 99%, and after that with the increase of solution pH (from 7 to 10), the ammonium removal efficiency decreased to 63%, which demonstrated that pH = 7 was the optimum pH. This finding was consistent with other reports.[1,26,27] It is known that there is competition between $H^+$ and $NH_4^+$ for exchange sites of 4A-molecular sieve, thus the removal efficiency of ammonium at pH < 7 was lower than the maximum (99%). When the concentration of $OH^-$ ions in solution increased, the percentage of molecular ammonia would increase and the surface of 4A-molecular sieve was blocked, which was not benefit for the ion exchange process.

In Fig. 4b, with the increase of pH from 2 to 4, the removal efficiency of HA by 4A-molecular sieve with single HA in the solution increased from 0 to 25%, thereafter, the removal efficiency decreased with the increase of pH. The HA has an electrostatic point (IEP) of about 1.9 and the HA molecules in the tested pH range were negatively charged because of the deprotonation of carboxyl groups or phenolic groups.[22] When pH was lower than the $pH_{zpc}$ of 4A-molecular sieve ($pH_{zpc}$ = 4.11), the surface of 4A-molecular sieve was positively charged which facilitated the HA adsorption. When pH was higher than the $pH_{zpc}$ of 4A-molecular sieve, the surface of adsorbent became negatively charged, which led to electrostatic repulsion interaction between the adsorbent and HA, and thus the reduction of the removal efficiency.

Fig. 4 also showed the effects of solution pH on the removal efficiency of ammonium and HA as binary components. The removal tendency of ammonium and HA was similar to that of single component of ammonium and HA, respectively, and the removal efficiency of both ammonium and HA was lower than that of single ammonium, while the removal of both ammonium and HA was higher than that of single HA. There are interactions among ammonium, HA and 4A-molecular sieve: (1) HA could adsorb a part of $NH_4^+$ by ion exchange process which could inhibit the adsorption of ammonium by 4A-molecular sieve; (2) HA are adsorbed by 4A-molecular sieve with the effects of hydrogen bonding, van der Waals force and cation-bridge,[28] and most of the adsorbed HA covers the surface, blocks some channels, and takes

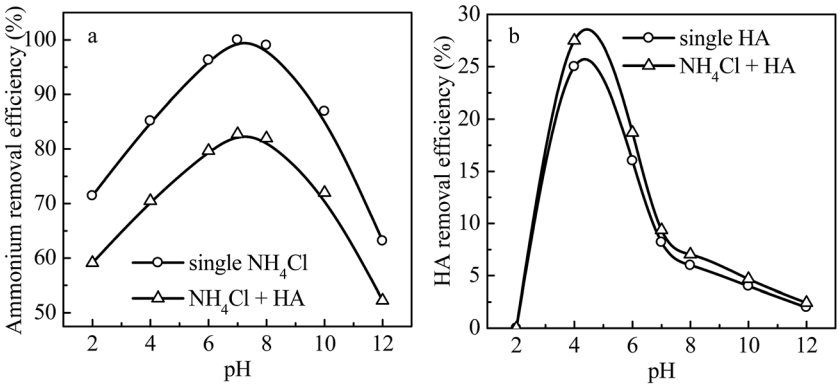


Fig. 4 Effects of solution pH on removal efficiency of (a) ammonium and (b) HA as both single and binary components by 4A-molecular sieve. (Conditions: temperature, 5 °C; $NH_4Cl$, 5 mg $L^{-1}$; HA, 2 mg $L^{-1}$; 4A-molecular sieve concentration, 1 g $L^{-1}$; contact time, 180 min; mixing speed, 200 rpm).

Open Access Article. Published on 17 March 2017. Downloaded on 10/17/2025 1:37:14 AM.
This article is licensed under a Creative Commons Attribution 3.0 Unported Licence.

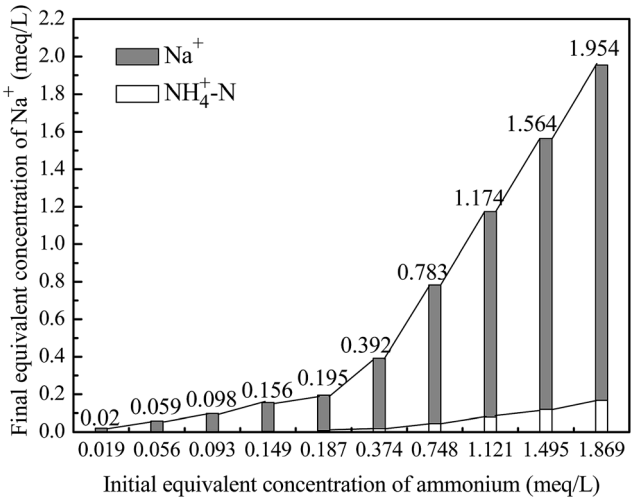


Fig. 5 Variation of equivalent concentrations of cations in the solution before and after reaction in the 4A-molecular sieve-solution system (conditions: temperature, 5 °C; pH 7; adsorbent concentration, 1 g $L^{-1}$; contact time, 180 min; mixing speed, 200 rpm).

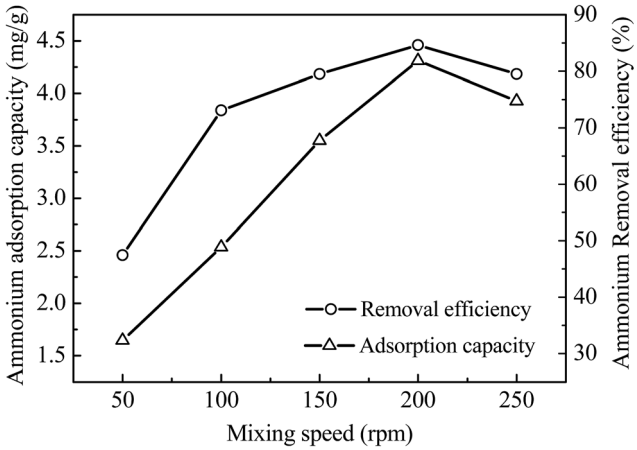


Fig. 6 The effects of mixing speed on adsorption capacity and removal efficiency of ammonium. (Conditions: temperature, 5 °C; pH 7; $NH_4Cl$, 5 mg $L^{-1}$; 4A-molecular sieve concentration, 1 g $L^{-1}$; contact time, 180 min).

up some adsorption sites of 4A-molecular sieve, which also inhibit the adsorption of ammonium; and (3) HA has surface activity which could reduce the surface tension of solution and consequently promotes the incompletely absorbed $NH_4^+$ to 4A-molecular sieve as well as facilitates its adsorption.[1] The interactions (1)–(3) could promote or inhibit the adsorption of ammonium. In Fig. 4, the removal efficiency of ammonium in the presence of HA was lower than that in the absence of HA, indicating that the presence of HA inhibited the adsorption of ammonium. The inhibition degree changed with the solution pH, and reached to the maximum at pH = 7. This can be explained by considering the difference in ionic charge of contaminants and the $pH_{zpc}$ of 4A-molecular sieve, as well as the difference in adsorption mechanism. The ammonium has been likely removed from solution through electrostatic attraction and ion-exchange,[29] which can be explained by variation of equivalent concentrations of cations in the solution before and after reaction in the 4A-molecular sieve-solution system given in Fig. 5. As shown in Fig. 5, the equivalent concentration of $Na^+$ in the solution increased after adsorption and the ion exchange amount of $Na^+$ and $NH_4^+$ accounted for more than 90% of the total ion exchange amount. Thus the deduced ion-exchange mechanism for ammonium removal by 4A-molecular sieve can be expressed below:

$$(\text{4A-molecular sieve-Na}^+) + NH_4^+ \rightarrow (\text{4A-molecular sieve-}NH_4^+) + Na^+ \quad (3)$$

The humic acid might be eliminated *via* mechanism of the electrostatic adsorption,[30] and the reaction was shown below:

$$(\text{4A-molecular sieve-Na}^+) + HA^- \rightarrow (\text{4A-molecular sieve-Na}^{\pm HA}) \quad (4)$$

Improvement of humic acid removal in the presence of ammonia was due to the cation-bridge effect,[30] which is the formation of a complex between functional phenolic and/or carboxylic groups in humic acid molecules with the ammonium ions adsorbed on the surface of 4A-molecular sieve. It can be expressed as the following equation:

$$(\text{4A-molecular sieve-}NH_4^+) + HA^- \rightarrow (\text{4A-molecular sieve-}NH_4^{\pm HA}) \quad (5)$$

### 3.5 The effects of mixing speed on adsorption

The effects of mixing speed (50, 100, 150, 200 and 250 rpm) on adsorption capacity and removal efficiency of ammonium by 4A-molecular sieve were also investigated in this study. As depicted in Fig. 6, the adsorption capacity and removal efficiency of ammonium increased with the increase of mixing speed and reached to a maximum at the mixing speed of 200 rpm. High mixing speed could quickly obtain a balance between contaminants and adsorbents, which elevated the ammonium removal significantly. But when the mixing speed was higher than 200 rpm (at 250 rpm), the removal efficiency was lower than that of 200 rpm, which indicated that the adsorption of 4A-molecular sieve was saturated at the mixing speed of 200 rpm.

### 3.6 The effects of initial contaminants' concentration on adsorption and adsorption isotherms

The influences of initial concentration of $NH_4Cl$ and HA on adsorption capacity as both single and binary contaminants were investigated in this study, and the results were shown in Fig. 7 and 8. With the increase of initial concentrations of contaminant(s), the adsorption capacities increased, however, the slopes of curves decreased which indicated that the removal efficiency of ammonium and HA decreased. It may be ascribed to the 4A-molecular sieve becoming saturated.[26]

The adsorption isotherm was also estimated to determine the maximum adsorption capacity of ammonium and HA by 4A-molecular sieve and to obtain the adsorption mechanisms.

Open Access Article. Published on 17 March 2017. Downloaded on 10/17/2025 1:37:14 AM.
This article is licensed under a Creative Commons Attribution 3.0 Unported Licence.

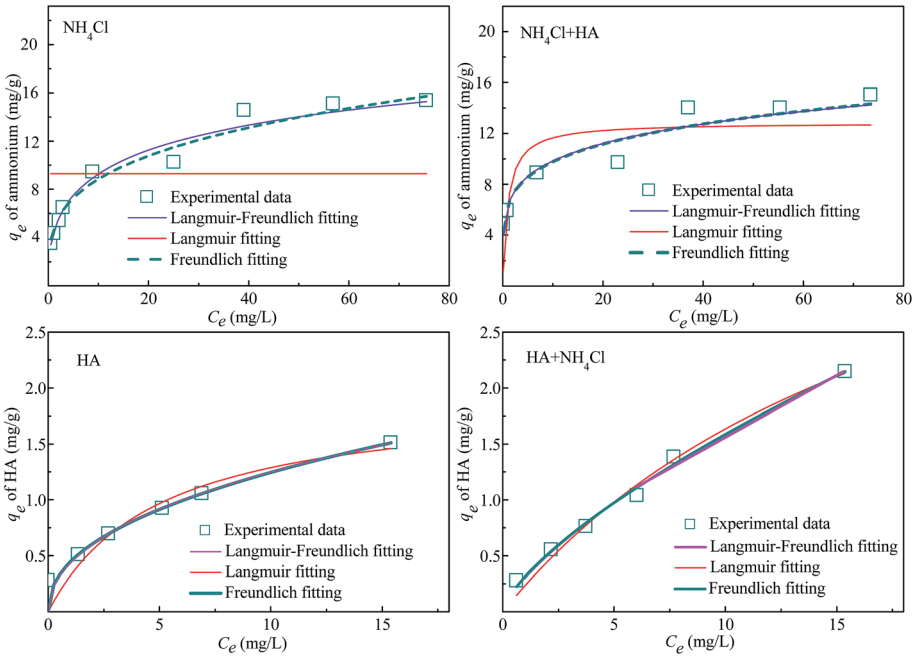


Fig. 7 Adsorption capacity as a function of concentration of $NH_4Cl$ and HA as single and binary components as well as the adsorption isotherms. (Conditions: pH 7; temperature, 5 °C; 4A-molecular sieve concentration, 1 g $L^{-1}$; mixing speed, 200 rpm; contact time, 180 min).

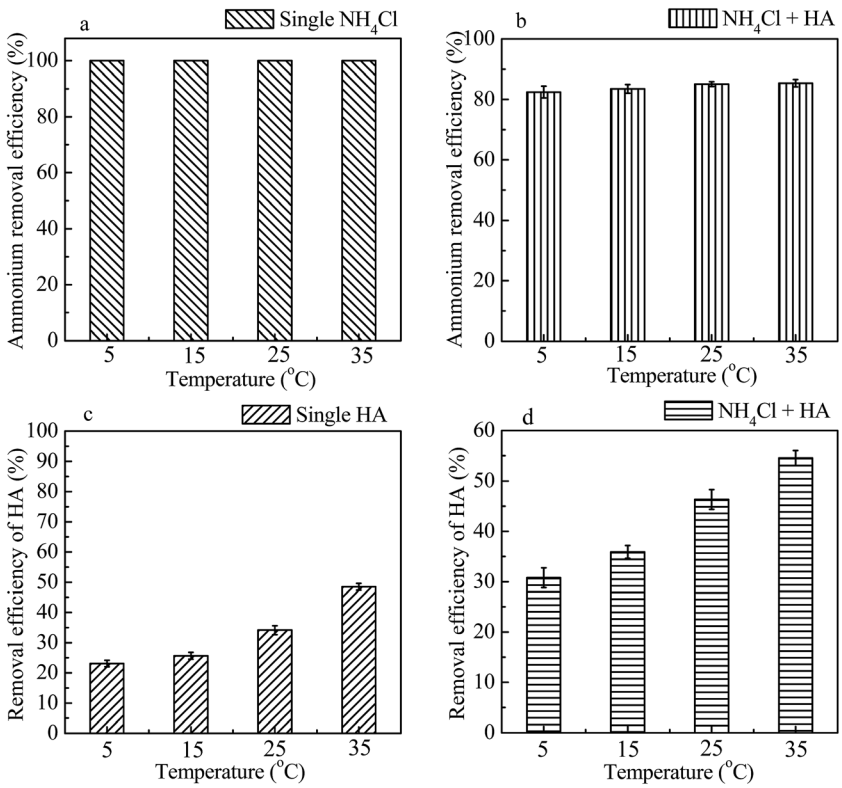


Fig. 8 Effects of temperature on removal efficiency of ammonium and HA by 4A molecular sieve with $NH_4Cl$ and HA as single and binary components. (Conditions: pH 7; $NH_4Cl$, 5 mg $L^{-1}$; HA, 2 mg $L^{-1}$; 4A-molecular sieve concentration, 1 g $L^{-1}$; contact time, 180 min).

 This journal is © The Royal Society of Chemistry 2017

Open Access Article. Published on 17 March 2017. Downloaded on 10/17/2025 1:37:14 AM.
This article is licensed under a Creative Commons Attribution 3.0 Unported Licence.

Table 4 Parameters of different absorption isotherm equations for HA and ammonium adsorption by 4A-molecular sieve with $NH_4Cl$ and HA as single and binary component at 5 °C

| | Ammonium adsorption | | | | | HA adsorption | | | | |
|---|---|---|---|---|---|---|---|---|---|---|
| | | Parameters | | | | | Parameters | | | |
| Equation | Component | $q_m$ | $b$ | | $R^2$ | Component | $q_m$ | $b$ | | $R^2$ |
| Langmuir | Single $NH_4Cl$ | 4.644 | 2.455 | | 0 | Single HA | 1.931 | 0.200 | | 0.897 |
| | Binary | 6.427 | 0.969 | | 0.661 | Binary | 4.913 | 0.050 | | 0.986 |
| | | $q_m$ | $b$ | $n$ | $R^2$ | | $q_m$ | $b$ | $n$ | $R^2$ |
| Langmuir-Freundlich | Single $NH_4Cl$ | 68.039 | 0.022 | 2.284 | 0.956 | Single HA | 14.559 | 0.031 | 2.081 | 0.918 |
| | Binary | 61.389 | 0.054 | 4.851 | 0.931 | Binary | 20.583 | 0.010 | 1.360 | 0.994 |
| | | $K_F$ | $1/n$ | | $R^2$ | | $K_F$ | $1/n$ | | $R^2$ |
| Freundlich | Single $NH_4Cl$ | 2.296 | 0.285 | | 0.961 | Single HA | 0.445 | 0.447 | | 0.918 |
| | Binary | 3.148 | 0.191 | | 0.933 | Binary | 0.314 | 1.421 | | 0.994 |

Freundlich, Langmuir and Langmuir–Freundlich equations were used to fit the experimental data, and the equations were expressed as below:

Freundlich equation:

$$q_e = K_F C_e^{1/n} \tag{6}$$

Langmuir equation:

$$q_e = \frac{b q_m C_e}{1 + b C_e} \tag{7}$$

and Langmuir–Freundlich equation:

$$q_e = \frac{b q_m C_e^{1/n}}{1 + b C_e^{1/n}} \tag{8}$$

where $K_F$ is Freundlich constant, $1/n$ is the heterogeneity factor, $q_m$ (mg $g^{-1}$) is the theoretical adsorption capacity of adsorbent for contaminant(s), and $b$ (L $mg^{-1}$) is Langmuir constant. The Langmuir equation is applied to homogeneous surface and the monolayer adsorption, while the Freundlich equation is applied to heterogeneous surface.[24]

The parameters of fitted curves were listed in Table 4. According to the values of $R^2$, the fitting degree of experimental data in three models can be evaluated. It was found that the

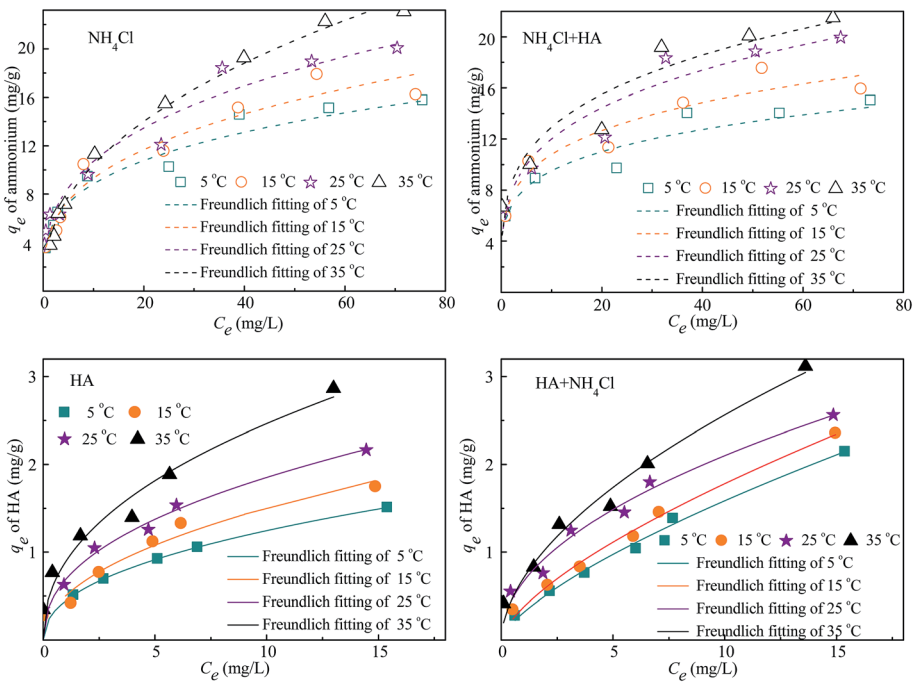


Fig. 9 The adsorption isotherms of ammonium and HA by 4A-molecular sieve as single and binary components at different temperature. (Conditions: pH 7; 4A-molecular sieve concentration, 1 g $L^{-1}$; mixing speed, 200 rpm; contact time, 180 min).

Open Access Article. Published on 17 March 2017. Downloaded on 10/17/2025 1:37:14 AM.
This article is licensed under a Creative Commons Attribution 3.0 Unported Licence.

values of $R^2$ in the Freundlich equation ($R^2$ between 0.918 and 0.994) were higher than those of other two equations, which indicated that the adsorption of ammonium and HA by 4A-molecular sieve was a multilayer system with non-uniform adsorption.[1] The mechanisms for simultaneous adsorption of ammonium and HA were also verified by the heterogeneity of 4A-molecular sieve surface and the multilayer adsorption system presented in Section 3.3. The values of $K_F$ for both single and binary component were much higher for adsorption of ammonium (from 2.296 to 3.148) than that of HA (from 0.445 to 0.314), showing that the 4A-molecular sieve was more appropriate for adsorption of ammonium compared to the adsorption of HA.[31]

### 3.7 The effects of temperature on adsorption and adsorption isotherms

The effects of temperature on removal efficiency of ammonium and/or HA by 4A-molecular sieve were studied and the results were depicted in Fig. 8. When the temperature increased from 5 to 35 °C, the removal efficiency of ammonium reached to 100% for single component and increased slightly with the presence of HA, whereas the removal efficiency of HA was increased less than 30%.

The adsorption capacity of ammonium and HA determined at different temperatures was fitted using Freundlich isotherms (shown in Fig. 9) and the parameters were listed in Table 5. With the increase of temperature from 5 to 35 °C, the values of $K_F$ for both single and binary component increased and at each specific temperature were higher for adsorption of ammonium (from 1.962 to 3.550) than for that of HA (from 0.314 to 0.891), proving that the 4A-molecular sieve had a higher affinity for ammonium adsorption, which was in consistent with the findings before (Section 3.4). When the temperature increased from 5 to 35 °C, the maximum adsorption capacity ($q_{e\text{-max}}$) of ammonium for single $NH_4Cl$ and both $NH_4Cl$ and HA increased from 68.039 to 173.163 mg g$^{-1}$ and from 61.389 to 169.738 mg g$^{-1}$, respectively, indicating that the addition of HA reduced the $q_{e\text{-max}}$ of ammonium. Meanwhile, the maximum adsorption capacity ($q_{e\text{-max}}$) of HA for single HA and both $NH_4Cl$ and HA increased from 14.559 to 16.534 mg g$^{-1}$ and from 20.583 to 27.444 mg g$^{-1}$, respectively, indicating that the addition of $NH_4Cl$ increased the $q_{e\text{-max}}$ of HA. This trend was similar to the results in Section 3.3 and 3.4. So far, there was no other reports available on simultaneous adsorption of ammonium and HA by 4A-molecular sieve, therefore no data could be used to compare the results of this study.

According to the results above, it was implied that the temperature did not have significant influences on adsorption by 4A-molecular sieve, thus high performance of ammonium and HA adsorption can be obtained even at low temperature, which was benefit for applications of 4A-molecular sieve in north of China.

### 3.8 Kinetics of adsorption

Adsorption kinetics of ammonium and HA onto 4A-molecular sieve at different initial concentration of contaminant(s) were also investigated in this study. Pseudo-first order kinetics and pseudo-second order kinetics which were usually applied to describe adsorption of organic pollutants onto adsorbents were used to fit the time-course experimental results, and the models were expressed as follows:

Pseudo-first-order equation:

$$\ln(q_e - q_t) = \ln q_e - k_1 t \tag{9}$$

Pseudo-second-order equation:

$$\frac{t}{q_t} = \frac{1}{k_2 q_e^2} + \frac{t}{q_2} \tag{10}$$

where $q_t$ (mg g$^{-1}$) is the adsorption capacity at time $t$ (min), $k_1$ and $k_2$ are constants of adsorption rate, $h = k_2 q_e^2$ equals to the rate of adsorption (mg (g$^{-1}$ min$^{-1}$)). The boundary conditions of two equations are $q_t = 0$ at $t = 0$ and $q_t = q_e$ at $t = t$.

The parameters of the fittings were summarized in Table 5 (the original data and fitting lines were shown in Fig. 10 and 11). Comparing the fitting degree ($R^2$) of the two models, it can be found that the pseudo-second order kinetics had better fitness

Table 5 Parameters of Freundlich isotherm equation for HA and ammonium adsorption by 4A-molecular sieve with $NH_4Cl$ and HA as single and binary component

| | | Ammonium adsorption | | | | | HA adsorption | | | | |
|---|---|---|---|---|---|---|---|---|---|---|---|
| Component | $T$ (°C) | $K_F$ | $1/n$ | $R^2$ | $q_{e\text{-max}}$ | $K_d$ | $K_F$ | $1/n$ | $R^2$ | $q_{e\text{-max}}$ | $K_d$ |
| Single $NH_4Cl$ | 5 | 2.296 | 0.285 | 0.961 | 68.039 | 0.09 | | | | | |
| | 15 | 2.199 | 0.326 | 0.953 | 96.205 | 0.10 | | | | | |
| | 25 | 2.505 | 0.330 | 0.963 | 126.900 | 0.14 | | | | | |
| | 35 | 1.962 | 0.425 | 0.992 | 173.163 | 0.15 | | | | | |
| Single HA | 5 | | | | | | 0.445 | 0.447 | 0.918 | 14.559 | 0.10 |
| | 15 | | | | | | 0.500 | 0.479 | 0.923 | 14.712 | 0.12 |
| | 25 | | | | | | 0.687 | 0.431 | 0.935 | 15.148 | 0.15 |
| | 35 | | | | | | 0.891 | 0.442 | 0.943 | 16.534 | 0.22 |
| $NH_4Cl$ + HA | 5 | 3.148 | 0.191 | 0.933 | 61.389 | 0.10 | 0.314 | 0.704 | 0.994 | 20.583 | 0.14 |
| | 15 | 3.180 | 0.230 | 0.919 | 89.120 | 0.11 | 0.375 | 1.477 | 0.992 | 24.335 | 0.16 |
| | 25 | 3.249 | 0.267 | 0.921 | 118.560 | 0.15 | 0.667 | 0.499 | 0.977 | 25.882 | 0.17 |
| | 35 | 3.550 | 0.261 | 0.908 | 169.738 | 0.16 | 0.705 | 0.561 | 0.977 | 27.444 | 0.23 |

 This journal is © The Royal Society of Chemistry 2017

Open Access Article. Published on 17 March 2017. Downloaded on 10/17/2025 1:37:14 AM.
This article is licensed under a Creative Commons Attribution 3.0 Unported Licence.

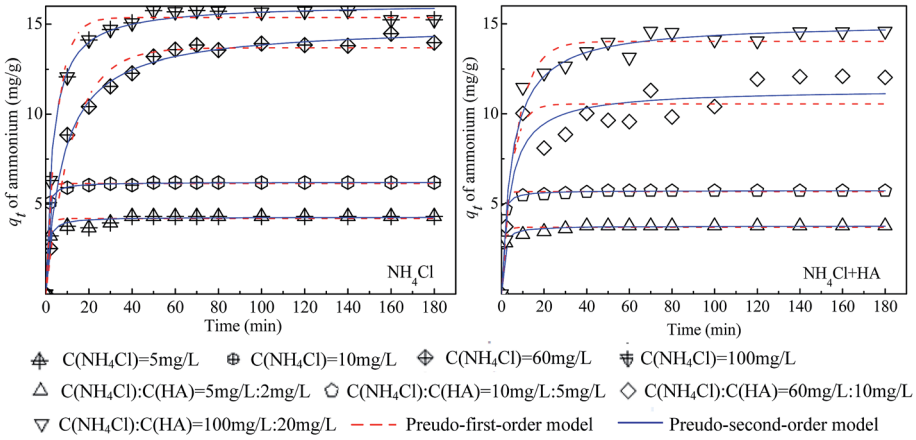


Fig. 10 Fitting curves of adsorption kinetics for ammonium adsorption by 4A-molecular sieve as single and binary components.

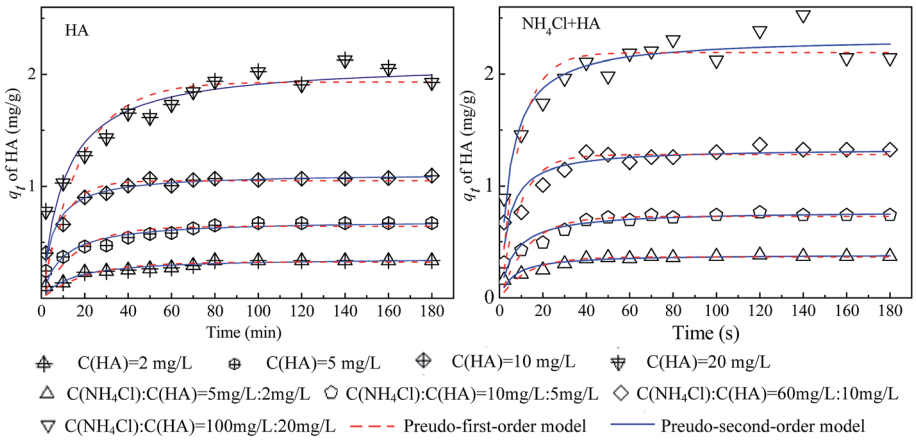


Fig. 11 Fitting curves of adsorption kinetics for ammonium adsorption by 4A-molecular sieve as single and binary components.

for adsorption of both ammonium and HA as single and binary components. With the increase of initial concentration of contaminants both for $NH_4Cl$ and HA as single and binary components, the constant value of pseudo-second order adsorption rate ($k_2$) decreased whereas the adsorption rate ($h$) increased gradually, which indicated that the mass transfer rate

Table 6 Parameters of adsorption kinetics for adsorption of ammonium and HA by 4A-molecular sieve

| Component | Concentration (mg $L^{-1}$) | Pseudo-first-order model | | | | Pseudo-second-order model | | | |
|---|---|---|---|---|---|---|---|---|---|
| | | $q_{e,exp}$ | $q_{e,model}$ | $k_1$ | $R^2$ | $q_{e,exp}$ | $k_2$ | $h(k_2q_e^2)$ | $R^2$ |
| Single | 5 | 4.311 | 4.192 | 0.733 | 0.960 | 4.276 | 0.308 | 5.623 | 0.979 |
| $NH_4Cl$ | 10 | 6.210 | 6.152 | 0.871 | 0.997 | 6.219 | 0.353 | 13.643 | 1.000 |
| | 60 | 13.968 | 13.683 | 0.081 | 0.982 | 13.917 | 0.094 | 18.205 | 0.995 |
| | 100 | 15.753 | 15.371 | 0.191 | 0.980 | 16.144 | 0.080 | 20.902 | 0.995 |
| $NH_4Cl$ + HA | 5 : 2 | 3.773 | 3.700 | 0.719 | 0.978 | 3.771 | 0.354 | 5.038 | 0.992 |
| | 10 : 5 | 5.734 | 5.684 | 0.872 | 0.997 | 5.746 | 0.379 | 12.513 | 0.999 |
| | 60 : 10 | 12.038 | 10.548 | 0.222 | 0.867 | 11.372 | 0.216 | 27.931 | 0.908 |
| | 100 : 20 | 14.588 | 14.024 | 0.139 | 0.979 | 15.056 | 0.136 | 30.829 | 0.981 |
| Single HA | 2 | 0.335 | 0.324 | 0.048 | 0.842 | 0.362 | 0.201 | 0.026 | 0.908 |
| | 5 | 0.671 | 0.642 | 0.063 | 0.789 | 0.698 | 0.159 | 0.078 | 0.903 |
| | 10 | 1.095 | 1.050 | 0.111 | 0.896 | 1.116 | 0.182 | 0.227 | 0.963 |
| | 20 | 2.127 | 1.932 | 0.056 | 0.758 | 2.109 | 0.046 | 0.204 | 0.860 |
| $NH_4Cl$ + HA | 5 : 2 | 0.381 | 0.364 | 0.078 | 0.779 | 0.388 | 0.404 | 0.061 | 0.874 |
| | 10 : 5 | 0.763 | 0.728 | 0.078 | 0.778 | 0.775 | 0.201 | 0.121 | 0.873 |
| | 60 : 10 | 1.323 | 1.278 | 0.111 | 0.623 | 1.334 | 0.194 | 0.346 | 0.805 |
| | 100 : 20 | 2.387 | 2.190 | 0.111 | 0.782 | 2.328 | 0.088 | 0.477 | 0.890 |

Open Access Article. Published on 17 March 2017. Downloaded on 10/17/2025 1:37:14 AM.
This article is licensed under a Creative Commons Attribution 3.0 Unported Licence.

Table 7 Values of film diffusion ($D_f$) and intraparticle diffusion($D_p$) coefficients for adsorption of ammonium and HA by 4A-molecular sieve

| Component | Concentration | | $k_f$ | | $D_f$ | | $k_p$ | | $D_p$ | |
|---|---|---|---|---|---|---|---|---|---|---|
| | $NH_4Cl$ | HA | Amm-onium | HA | Amm-onium | HA | Amm-onium | HA | Amm-onium | HA |
| Single $NH_4Cl$ | 5 | | 0.687 | | 7.31E-8 | | 1.42E-5 | | 3.29E-13 | |
| | 10 | | 0.849 | | 6.50E-8 | | 1.46E-5 | | 3.37E-13 | |
| | 60 | | 0.075 | | 2.16E-9 | | 1.29E-5 | | 2.99E-13 | |
| | 100 | | 0.172 | | 3.34E-9 | | 1.37E-5 | | 3.17E-13 | |
| Single HA | | 2 | | 0.043 | | 8.84E-10 | | 1.21E-5 | | 2.79E-13 |
| | | 5 | | 0.053 | | 8.77E-10 | | 1.25E-5 | | 2.88E-13 |
| | | 10 | | 0.094 | | 1.27E-9 | | 1.31E-5 | | 3.03E-13 |
| | | 10 | | 0.039 | | 1.03E-9 | | 1.17E-5 | | 2.70E-13 |
| Binary | 5 | 2 | 0.688 | 0.066 | 6.40E-8 | 1.54E-9 | 1.44E-5 | 1.27E-5 | 3.32E-13 | 2.95E-13 |
| | 10 | 5 | 0.852 | 0.065 | 6.02E-8 | 1.23E-9 | 1.46E-5 | 1.27E-5 | 3.37E-13 | 2.95E-13 |
| | 60 | 10 | 0.084 | 0.094 | 2.09E-9 | 1.54E-9 | 1.23E-5 | 1.33E-5 | 2.85E-13 | 3.07E-13 |
| | 100 | 10 | 0.121 | 0.074 | 2.17E-9 | 2.17E-9 | 1.32E-5 | 1.25E-5 | 3.05E-13 | 2.90E-13 |

of contaminants onto the surface of 4A-molecular sieve was elevated. As seen in Table 6, the values of $k_2$ for binary adsorption of ammonium and HA were higher than that of single contaminant adsorption, which can be explained by the eqn (5) that the formation of new adsorption sites improved the mass transfer rate for simultaneous adsorption of ammonium and HA.

The adsorption kinetics were further investigated by fitting the experimental data with the intraparticle diffusion model shown as below:

$$q_t = k_{int} t^{1/2} + c \tag{11}$$

where $k_{int}$ is the coefficient of intraparticle diffusion (mg ($g^{-1}$ $min^{-0.5}$)).

Two or more linear relationships were found in the plots of intraparticle diffusion model for both ammonium and HA as single and binary components (not shown), which indicated that both intraparticle diffusion and film diffusion were involved in the adsorption processes.[1,32] The coefficients of intraparticle diffusion ($D_p$) and film diffusion ($D_f$) were calculated to determine the rate controlling steps in adsorption processes according to the equations as follows:

Intraparticle diffusion models:

$$\ln\left(1 - \left(\frac{q_t}{q_e}\right)^2\right) = -2k_p t \tag{12}$$

Film diffusion models:

$$\ln\left(1 - \frac{q_t}{q_e}\right) = -k_f t \tag{13}$$

where $k_p = D_p\pi^2/r^2$ and $k_f = D_f C/C_Z hr$ are rate constants, $C$ and $C_Z$ (mg $kg^{-1}$) are concentrations of contaminants in the solution and in the adsorbent, respectively, $h$ is the thickness of film on the surface of adsorbent, and $r$ (m) is the average particle radium of 4A-molecular sieve.

The values of $D_f$ and $D_p$ for adsorption of ammonium and HA by 4A-molecular sieve as single and binary components were listed in Table 7. It has been reported that the values of $D_f$ are in the range from $10^{-6}$ to $10^{-8}$ $cm^2$ $s^{-1}$ for the film diffusion controlling steps, while the values of $D_p$ ranged from $10^{-11}$ to $10^{-13}$ $cm^2$ $s^{-1}$ for the intraparticle diffusion controlling steps.[32] As seen from the Table 6, the $D_f$ was in the range of $10^{-8}$~$10^{-10}$ $cm^2$ $s^{-1}$ and $D_p$ was in the range of $10^{-12}$–$10^{-13}$, which revealed that the intraparticle diffusion was the dominant controlling step for adsorption of ammonium and HA by 4A-molecular sieve as single and binary components.

## 4. Conclusion

This study investigated the 4A-molecular sieve modified from ATP on adsorption capacity and removal efficiency of ammonium and HA as single and binary components. The influences of concentration of 4A-molecular sieve, pH values, mixing speed, initial contaminants' concentration, solution temperature and adsorption time on removal of ammonium and HA

 This journal is © The Royal Society of Chemistry 2017

Open Access Article. Published on 17 March 2017. Downloaded on 10/17/2025 1:37:14 AM.
This article is licensed under a Creative Commons Attribution 3.0 Unported Licence.

were thoroughly evaluated in this study. From the experimental results, it can be concluded that:

First, the removal efficiency of ammonium increased dramatically after alkali modification of ATP, while the removal of HA decreased.

Second, the Freundlich isotherm model was selected as the best model for the temperature evaluation and the temperature did not have significant influences on removal of ammonium and HA.

Accordingly, the 4A-molecular sieve modified from ATP was found to be an efficient adsorbent for removal of ammonium even at low temperature. The experimental data provided in this study was considered useful for applications of ATP and 4A-molecular sieve.

## Acknowledgements

This work was supported by Science and Technology Research Project of Education Department of Heilongjiang Province, China (12531034), and Science and Technology Innovation Talents Project of Harbin (2016RQQXJ092).

## References

1 G. Moussavi, S. Talebi, M. Farrokhi and R. M. Sabouti, The investigation of mechanism, kinetic and isotherm of ammonia and humic acid co-adsorption onto natural zeolite, *Chem. Eng. J.*, 2011, **171**, 1159–1169.

2 X. Huang, W. Li, D. Zhang and W. Qin, Ammonium removal by a novel oligotrophic Acinetobacter sp. Y16 capable of heterotrophic nitrification–aerobic denitrification at low temperature, *Bioresour. Technol.*, 2013, **146**, 44–50.

3 F. mazloomi and M. jalali, Ammonium removal from aqueous solutions by natural Iranian zeolite in the presence of organic acids, cations and anions, *J. Environ. Chem. Eng.*, 2016, **4**, 1664–1673.

4 D. Zhang, W. Li, X. Huang and W. Qin, Removal of ammonium in surface water at low temperature by a newly isolated Microbacterium sp. strain SFA13, *Bioresour. Technol.*, 2013, **137**, 147–152.

5 R. Sudoh, M. S. Islam, K. Sazawa and T. Okazaki, Removal of dissolved humic acid from water by coagulation method using polyaluminum chloride (PAC) with calcium carbonate as neutralizer and coagulant aid, *J. Environ. Chem. Eng.*, 2015, **3**, 770–774.

6 K. Szymański, A. W. Morawski and S. Mozia, Humic acids removal in a photocatalytic membrane reactor with a ceramic UF membrane, *Chem. Eng. J.*, 2016, **305**, 19–27.

7 P. Kanagaraj, A. Nagendran, D. Rana and T. Matsuura, Separation of macromolecular proteins and removal of humic acid by cellulose acetate modified UF membranes, *Int. J. Biol. Macromol.*, 2016, **89**, 81–88.

8 T. Wang, G. Qu, J. Ren and Q. Yan, Evaluation of the potentials of humic acid removal in water by gas phase surface discharge plasma, *Water Res.*, 2016, **89**, 28–38.

9 Y. He, H. Lin, Y. Dong and Q. Liu, Simultaneous removal of ammonium and phosphate by alkaline-activated and lanthanum-impregnated zeolite, *Chemosphere*, 2016, **164**, 387–395.

10 M. Li, C. Feng, Z. Zhang and X. Lei, Simultaneous regeneration of zeolites and removal of ammonia using an electrochemical method, *Microporous Mesoporous Mater.*, 2010, **127**, 161–166.

11 L. Lin, Z. Lei, L. Wang and X. Liu, Adsorption mechanisms of high-levels of ammonium onto natural and NaCl-modified zeolites, *Sep. Purif. Technol.*, 2013, **103**, 15–20.

12 L. Wang, C. Han, M. N. Nadagouda and D. D. Dionysiou, An innovative zinc oxide-coated zeolite adsorbent for removal of humic acid, *J. Hazard. Mater.*, 2016, **313**, 283–290.

13 S. Wang and Y. Peng, Natural zeolites as effective adsorbents in water and wastewater treatment, *Chem. Eng. J.*, 2010, **156**, 11–24.

14 T. S. Anirudhan, P. S. Suchithra and S. Rijith, Amine-modified polyacrylamide–bentonite composite for the adsorption of humic acid in aqueous solutions, *Colloids Surf., A*, 2008, **326**, 147–156.

15 D. Doulia, C. Leodopoulos, K. Gimouhopoulos and F. Rigas, Adsorption of humic acid on acid-activated Greek bentonite, *J. Colloid Interface Sci.*, 2009, **340**, 131–141.

16 M. Salman, B. El-Eswed and F. Khalili, Adsorption of humic acid on bentonite, *Appl. Clay Sci.*, 2007, **38**, 51–56.

17 Z. Sun, X. Qu, G. Wang and S. Zheng, Removal characteristics of ammonium nitrogen from wastewater by modified Ca-bentonites, *Appl. Clay Sci.*, 2015, **107**, 46–51.

18 X. Ji, M. Zhang, Y. Wang and Y. Song, Immobilization of ammonium and phosphate in aqueous solution by zeolites synthesized from fly ashes with different compositions, *J. Ind. Eng. Chem.*, 2015, **22**, 1–7.

19 S. Wang, T. Terdkiatburana and M. O. Tadé, Single and co-adsorption of heavy metals and humic acid on fly ash, *Sep. Purif. Technol.*, 2008, **58**, 353–358.

20 A. A. M. Daifullah, B. S. Girgis and H. M. H. Gad, A study of the factors affecting the removal of humic acid by activated carbon prepared from biomass material, *Colloids Surf., A*, 2004, **235**, 1–10.

21 X. Zhang and R. Bai, Mechanisms and kinetics of humic acid adsorption onto chitosan-coated granules, *J. Colloid Interface Sci.*, 2003, **264**, 30–38.

22 J. Wang, X. Han, H. Ma, Y. Ji and L. Bi, Adsorptive removal of humic acid from aqueous solution on polyaniline/attapulgite composite, *Chem. Eng. J.*, 2011, **173**, 171–177.

23 J. Zhang, S. Xie and Y.-S. Ho, Removal of fluoride ions from aqueous solution using modified attapulgite as adsorbent, *J. Hazard. Mater.*, 2009, **165**, 218–222.

24 J. Huang, Y. Liu and X. Wang, Selective adsorption of tannin from flavonoids by organically modified attapulgite clay, *J. Hazard. Mater.*, 2008, **160**, 382–387.

25 J. Jiang, L. Feng, X. Gu and Y. Qian, Synthesis of zeolite A from palygorskite *via* acid activation, *Appl. Clay Sci.*, 2012, **55**, 108–113.

26 H. Huang, X. Xiao, B. Yan and L. Yang, Ammonium removal from aqueous solutions by using natural Chinese (Chende) zeolite as adsorbent, *J. Hazard. Mater.*, 2010, **175**, 247–252.

Open Access Article. Published on 17 March 2017. Downloaded on 10/17/2025 1:37:14 AM.
This article is licensed under a Creative Commons Attribution 3.0 Unported Licence.

27 K. Saltalı, A. Sarı and M. Aydın, Removal of ammonium ion from aqueous solution by natural Turkish (Yıldızeli) zeolite for environmental quality, *J. Hazard. Mater.*, 2007, **141**, 258–263.
28 S.-j. Park and T.-i. Yoon, Effects of iron species and inert minerals on coagulation and direct filtration for humic acid removal, *Desalination*, 2009, **239**, 146–158.
29 A. A. Ismail, R. M. Mohamed, I. A. Ibrahim and G. Kini, Synthesis, optimization and characterization of zeolite A and its ion-exchange properties, *Colloids Surf., A*, 2010, **366**, 80–87.
30 S. Capasso, S. Salvestrini, E. Coppola and A. Buondonno, Sorption of humic acid on zeolitic tuff: a preliminary investigation, *Appl. Clay Sci.*, 2005, **28**, 159–165.
31 Y. Zhao, B. Zhang, X. Zhang and J. Wang, Preparation of highly ordered cubic NaA zeolite from halloysite mineral for adsorption of ammonium ions, *J. Hazard. Mater.*, 2010, **178**, 658–664.
32 V. Vadivelan and K. V. Kumar, Equilibrium, kinetics, mechanism, and process design for the sorption of methylene blue onto rice husk, *J. Colloid Interface Sci.*, 2005, **286**, 90–100.

 This journal is © The Royal Society of Chemistry 2017